



HAL
open science

Challenging development of storable particles for oral delivery of a physiological nitric oxide donor

Yi Zhou, Caroline Gaucher, Isabelle Fries, Mehmet-Akif Hobekkaya, Charlène Martin, Clément Leonard, Frantz Deschamps, Anne Sapin-Minet, Marianne Parent

► To cite this version:

Yi Zhou, Caroline Gaucher, Isabelle Fries, Mehmet-Akif Hobekkaya, Charlène Martin, et al.. Challenging development of storable particles for oral delivery of a physiological nitric oxide donor. Nitric Oxide: Biology and Chemistry, 2020, 104-105, pp.1-10. 10.1016/j.niox.2020.08.001 . hal-02922699

HAL Id: hal-02922699

<https://hal.univ-lorraine.fr/hal-02922699>

Submitted on 24 Aug 2022

HAL is a multi-disciplinary open access archive for the deposit and dissemination of scientific research documents, whether they are published or not. The documents may come from teaching and research institutions in France or abroad, or from public or private research centers.

L'archive ouverte pluridisciplinaire **HAL**, est destinée au dépôt et à la diffusion de documents scientifiques de niveau recherche, publiés ou non, émanant des établissements d'enseignement et de recherche français ou étrangers, des laboratoires publics ou privés.



Distributed under a Creative Commons Attribution - NonCommercial 4.0 International License

Challenging development of storable particles for oral delivery of a physiological nitric oxide donor

Yi ZHOU^a, Caroline GAUCHER^a, Isabelle FRIES^a, Mehmet-Akif HOBEKKAYA^a, Charlène MARTIN^a, Clément LEONARD^b, Frantz DESCHAMPS^b, Anne SAPIN-MINET^a, Marianne PARENT^{a,*}

^a Université de Lorraine, CITHEFOR, F-54000 Nancy, France

^b StaniPharm, 5 rue Jacques Monod, BP 10, 54250 Champigneulles, France

*Correspondence: marianne.parent@univ-lorraine.fr, EA 3452 CITHEFOR, Campus Brabois Santé, 9 avenue de la Forêt de Haye - BP 20199, 54505 Vandoeuvre Les Nancy Cedex, Tel +33-3-7274-7307

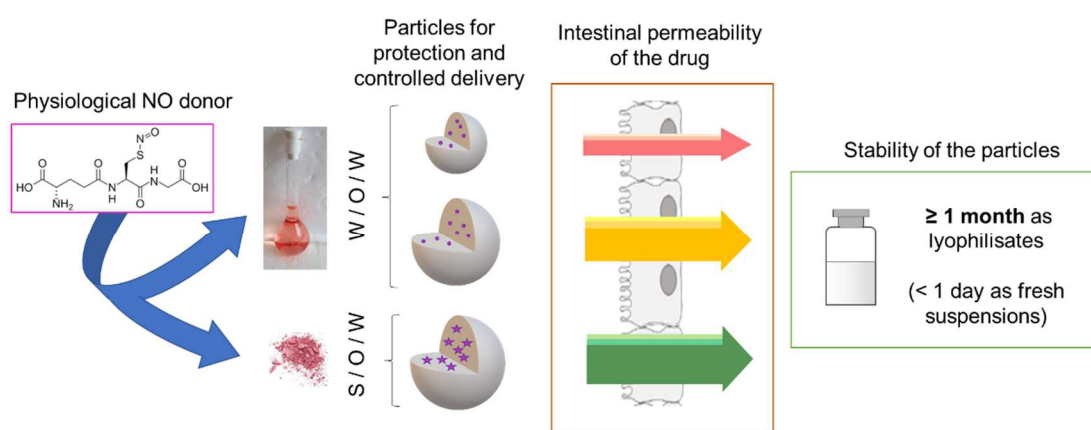
Mr Yi ZHOU was supported by a CSC (China Scholarship Council) funding.

The authors acknowledge support of EA 3452 CITHEFOR by the “Impact Biomolecules” project of the “Lorraine Université d’Excellence” (Investissements d’avenir – ANR).

These funding sources were not involved in study design, collection, analysis, interpretation of data, writing of the report nor in the decision to submit it for publication.

Declarations of interest: none

Graphical Abstract:



Abstract:

Nitric oxide (NO) deficiency is often associated with several acute and chronic diseases. NO donors and especially *S*-nitrosothiols such as *S*-nitrosoglutathione (GSNO) have been identified as promising therapeutic agents. Although their permeability through the intestinal barrier have recently be proved, suitable drug delivery systems have to be designed for their oral administration. This is especially challenging due to the physico-chemical features of these drugs: high hydrophilicity and high lability. In this paper, three types of particles were prepared with an Eudragit polymer: nanoparticles and microparticles obtained with a water-in-oil-in-water emulsion/evaporation process *versus* microparticles obtained with a solid-in-oil-in-water emulsion/evaporation process. They had a similar encapsulation efficiency (around 30%), and could be freeze-dried then be stored at least one month without modification of their critical attributes (size and GSNO content). However, microparticles had a slightly slower *in vitro* release of GSNO than nanoparticles, and were able to boost by a factor of two the drug intestinal permeability (Caco-2 model). Altogether, this study brings new data about GSNO intestinal permeability and three ready-to-use formulations suitable for further preclinical studies with oral administration.

Keywords: nitric oxide, *S*-nitrosoglutathione, nanoparticles, microparticles, oral delivery

Highlights:

- GSNO is a promising drug, but challenging to formulate (hydrophilicity, lability)
- Nano and microparticles suitable for GSNO oral delivery were produced and compared
- Their critical attributes were maintained after freeze-drying and stable upon storage
- They improved the drug permeability through a Caco-2 model of intestinal barrier

1 1. Introduction

2 Nitric oxide (NO) is a radical messenger with a variety of physiological roles, *e.g.* control of vascular
3 tone, neurotransmission at both central and peripheral levels, mediation of immune response,
4 wound healing, tissue regeneration and anti-cancer defense [1]. As a result of these pleiotropic
5 actions, many pathological conditions are accompanied by a NO deficiency (*e.g.* atherosclerosis,
6 pulmonary hypertension, thrombosis, ischemia... [2-5]). As these conditions are becoming
7 increasingly frequent in the population with ageing, a treatment able to restore the physiological NO
8 levels would represent a major therapeutic advance for a growing number of patients.

9 NO itself cannot be used directly in many cases because of its very short half-life (< 1 s) [6].
10 Moreover, its gaseous nature makes it difficult to store, to transport and to administer. In this
11 context, NO donors have been developed over the past decades, including organic nitrates [7-8],
12 nitrosamines [9], metal-NO complexes [10], diazenium-diolates (NONOates, [11]) and S-nitrosothiols
13 (RSNO, [12-13]). As RSNO are the physiologic forms of NO transport and storage in our body, they are
14 considered as “hot candidates” with no efficacy nor toxicity concerns. In particular, S-
15 nitrosoglutathione (GSNO) has gained a lot of attention in preclinical and clinical trials for different
16 biomedical applications [14-15]. GSNO is a physiological low-molecular-weight RSNO, with
17 arterioselective vasodilating and antiplatelet effects. Additionally, the NO moiety in GSNO is grafted
18 to glutathione (GSH), which is the main redox buffer with antioxidant properties in our cells. Thus,
19 GSNO will release both NO and GSH: this could be beneficial as NO deficiency is generally associated
20 to oxidative stress in many conditions. However, pharmacokinetics data are drastically limited by the
21 fact that GSNO is a very hydrophilic (clogP = - 2.7) and labile active drug, highly reactive to its
22 environment. GSNO is rapidly degraded or metabolized by several (*e.g.* protein disulfide isomerases
23 [16], thioredoxins [17], GSNO reductase [18], gamma-glutamyl transpeptidase [19]). RSNO
24 metabolism leads to the formation of multiple NO-derived species (NO_x, including nitrite and nitrate
25 ions), therefore difficult to follow throughout the entire organism. Only few studies have attempted
26 to define RSNO pharmacokinetic parameters, especially after oral administration, as this require
27 technically demanding methods (radioisotope tracking of NO [20-21]). Furthermore, little is known
28 on the crossing of the intestinal barrier by RSNO. Bonetti et al. [22] revealed the ability of 3 RSNO
29 (including GSNO) to cross the intestinal barrier (Caco-2 model) with a medium apparent permeability
30 rate, using a passive mode. As the therapeutic effects of NO depend not only on the location of
31 production/release, but also on the rate and quantity of available NO, it is a real pharmaceutical
32 challenge to propose a formulation of GSNO able to protect and to deliver it properly. As already
33 mentioned, to the great distress of formulators, GSNO is very sensitive: to light, oxygen, heat, pH
34 changes, or presence of thiols or metallic ions even at low concentrations. As a drug, GSNO can be
35 stored only as powder, at -20°C, protected from light and under an inert atmosphere. Precautions
36 (ultrapure water, light protection) have to be taken to prepare GSNO solutions, which should be
37 discarded after few hours. These characteristics make it very challenging and raise many hurdles to
38 develop GSNO formulations adapted to oral delivery, the most attractive route of administration to
39 manage patients in the context of chronic diseases.

40 Among the few examples in the literature, conjugation of GSNO to diblock polymers was proposed
41 [23] as well as direct encapsulation of GSNO into various hydrophilic (alginate, chitosan...) or
42 hydrophobic polymeric matrices [24-29]. Hydrophilic polymers have generally less standardized
43 characteristics because of their natural origin. Their hydrophilic nature is favorable for GSNO
44 encapsulation, but the resulting loose hydrogels might lead to a fast drug release. Among
45 hydrophobic polymers, the Eudragit ones are especially interesting, as they are mucoadhesive
46 excipients already approved for human oral administration.

47 Wu et al. [30] used Eudragit RLPO, commonly used for tablet coating, to prepare nanoparticles which
48 were incorporated into an alginate/chitosan matrix to enhance GSNO loading and release profile
49 [31]. The resulting composite microparticles generated a NO store in rat aorta after a single oral
50 administration [32]. Despite of these very interesting results, the preclinical development of these
51 composites formulations is hindered by several points. First, the multi-step preparation and the
52 adequate characterization are too time-consuming. Second, these formulations are not stable and
53 should be used immediately after preparation (no possibility to be sent to other labs to be tested in
54 preclinical models).

55 Following these precedents, the aims of this work were to: (i) propose a new drug delivery system
56 that enables GSNO stabilization and controlled release; (ii) provide information on GSNO intestinal
57 absorption from these developed delivery systems.

58 To overcome these barriers, GSNO-loaded Eudragit RLPO particles adapted for oral delivery were
59 prepared, with a reasonably simple protocol, at least similar encapsulation efficiency and release
60 profile than the previously described particles, and with a sufficient stability to be stored and/or sent
61 before use. According to the hydrophilic nature of the drug, microparticles (MP) were prepared by
62 double emulsion/solvent evaporation, either with a water-in-oil-in water (W/O/W) process (GSNO-
63 MPW) or a solid-in-oil-in-water (S/O/W) process (GSNO-MPS). They were compared to nanoparticles
64 obtained with a W/O/W process (GSNO-NP) in terms of size, encapsulation efficiency and *in vitro*
65 release. Moreover, to get particles in a stable solid state, a lyophilization process was applied.
66 Potential modifications of critical product attributes (GSNO content and particle size) were assessed
67 immediately after lyophilization and during refrigerated storage. Afterwards, the cytocompatibility of
68 the particles was evaluated on Caco-2 cells. Finally, intestinal permeability of NO_x species was
69 evaluated using an *in vitro* model of intestinal barrier.

70

71 **2. Material and methods**

72 All solutions were prepared with ultrapure deionized water (> 18.2 MΩ.cm). GSNO powder was
73 synthesized, purified and stored as previously described [31]. Eudragit® RLPO was a gift from Evonik
74 industries (Germany). HgCl₂ was purchased from Prolabo (Switzerland), NaNO₂ from Merck
75 (Germany), NaOH from VWR Chemicals (Czech Republic), methanol from Carlo Erba Reagents
76 (France). All other reagents were obtained from Sigma–Aldrich (France).

77 **2.1. GSNO powder synthesis**

78 GSNO powder was synthesized, purified and stored as previously described [33]. Briefly, sodium
79 nitrite and reduced glutathione (GSH), equivalent amount, were incubated under acidic condition
80 (0.626 M HCl). The solid form of GSNO was obtained by cold acetone precipitation, then washed,
81 dried under vacuum and stored at -20°C under inert dinitrogen atmosphere. GSNO purity > 95% is
82 required for batch release (see [33] for details about control).

83 **2.2 Quantification of GSNO, nitrite ions and nitrate ions**

84 Nitrite ions and GSNO were quantified using a colorimetric (Griess and Griess-Saville reactions) or a
85 fluorimetric method (diaminonaphthalen (DAN) and DAN-Hg²⁺) with standard curves of sodium
86 nitrite and GSNO, respectively. Briefly, N₂O₃ generated from acidified nitrite ions reacts with Griess
87 reagent (Sulfanilamide and N-(1-naphthyl)ethylenediamine) or DAN in the presence (for GSNO) or
88 absence (for nitrite ions) of HgCl₂ producing a diazonium salt or 2,3-naphthotriazole that either
89 absorbs at 540 nm or emits fluorescence at 415 nm after excitation at 375 nm (JASCO FP-8300,

90 France). GSNO concentration was obtained by subtracting Griess to Griess-Saville quantification or
 91 DAN to DAN-Hg²⁺ quantification. Nitrate ions quantification (using a standard curve of sodium
 92 nitrate) included a reduction step of nitrate in nitrite ions using a nitrate reductase and its cofactors
 93 before the addition of DAN reagent (fluorometric kit nitrite/nitrate Cayman Chemical Ref. 780051,
 94 USA). Nitrate concentration was obtained by subtracting DAN-Hg²⁺ quantification to nitrate
 95 quantification using nitrate reductase.

96 2.3. Preparation and lyophilization of GSNO-loaded particles

97 2.3.1. Preparation of GSNO-loaded nanoparticles and microparticles

98 GSNO-loaded nanoparticles (GSNO-NP) were prepared by a water-in-oil-in-water (W/O/W)
 99 emulsion/solvent evaporation technique [30]. Briefly, 500 µL of 0.1% (w/v) Kolliphor P188 solution
 100 containing 10 mg of GSNO was emulsified by sonication for 60 s (11 W, 100% amplitude, Vibra cell™
 101 72434, France) in 5 mL of methylene chloride containing 500 mg of Eudragit, over an ice bath. The
 102 resulting primary emulsion was then poured in 19.5 mL of 0.1% (w/v) Kolliphor P188 solution with
 103 ultrasonication (30 W, amplitude maximum, Vibra cell™ 75022, France) for 30 s, to get the W/O/W
 104 emulsion. The final GSNO-NP suspension was obtained after 10 min of solvent evaporation.

105 GSNO-loaded microparticles were prepared by W/O/W process (GSNO-MPW) or by S/O/W process
 106 (GSNO-MPS). GSNO-MPW preparation followed the same process as GSNO-NP, except for the second
 107 emulsification, which was performed with a vortex (VV3, VWR, USA) at maximum speed for 60 s,
 108 rather than with ultrasonication. The whole process was conducted at controlled temperature (24 ±
 109 0.5 °C). GSNO-MPS were prepared as GSNO-MPW, except that 10 mg of GSNO powder (sieved at
 110 40 µm) were directly suspended in the Eudragit/DCM solution. Attempts to reduce the size of GSNO
 111 powder grain were made with supercritical fluid technology (see Table 1).

112 **Table 1. Conditions used in supercritical trials to decrease the size of GSNO powder grains.** Gaseous
 113 antisolvent (GAS) and supercritical antisolvent (SAS) processes rely on the use of the supercritical CO₂
 114 as an anti-solvent. The crystallization of GSNO is induced by the mass transfer of the solvent (DMSO)
 115 in the supercritical phase.

Treatment	Crystallization conditions	Drying conditions
GAS	Crystallization pressure: 300 bar Crystallization temperature: 40°C GSNO 1% wt in DMSO 10.9 g of solution injected CO ₂ pressurization: 150 bar/min Equilibrium: agitation 54 rpm 10 min before drying 20 mL autoclave	300 bar/40°C CO ₂ flow rate: 0.6 kg/h Duration: 3 h
SAS (1 st trial)	Crystallization pressure: 300 bar Crystallization temperature: 40°C GSNO 1% wt in DMSO 15.8 g of solution injected Molar CO ₂ fraction: 0.984 2.2 kg _{CO2} /h – 1.0 g _{sol} /min Coaxial nozzle (100 µm i.d.) 300 mL autoclave	300 bar/40°C CO ₂ flow rate: 1.0 kg/h Duration: 2 h 30

	Crystallization pressure: 160 bar	
	Crystallization temperature: 40°C	
	GSNO 1% wt in DMSO	
SAS	22.1 g of solution injected	160 bar/40°C
(2 nd trial)	Molar CO ₂ fraction: 0.971	CO ₂ flow rate: 1.1 kg/h
	1.1 kg _{CO2} /h – 1.0 g _{sol} /min)	Duration: 3 h
	Coaxial nozzle (130 μm i.d.)	
	300 mL autoclave	

116

117 **2.3.2. Lyophilization of GSNO-loaded particles**

118 After particles preparation, the suspensions were centrifuged (42,000 g, 4°C, 30 min for NP or 10 min
 119 for MP) and the pellets were re-suspended in 10 mL of 10% (w/v) sucrose solution. The re-
 120 suspensions were frozen at -80°C for 15 h ± 1 h then lyophilized for 24 h ± 1 h (FreeZone6
 121 LABCONCO USA, setups: condenser at -50°C and pressure at 0.04 mbar). A preliminary study was
 122 conducted to optimize the lyophilization of GSNO-NP and to select the best and lowest-cost
 123 conditions such as -80 °C freezing of the particles (instead of liquid nitrogen) and using sucrose as
 124 protectant (instead of trehalose, and no mannitol). The residual water content in the lyophilizate was
 125 immediately tested after freeze-drying using a Karl-Fischer apparatus (756 KF coulometer, France).
 126 All powders were placed under nitrogen and stored at 4°C protected from light.

127

128 **2.4. Physicochemical characterization of particles**

129 The hydrodynamic diameter, polydispersity index (PDI) and zeta-potential of the GSNO-NP were
 130 measured in triplicate in 1 mM NaCl by dynamic light scattering (Zetasizer Nano ZS, Malvern
 131 Instrument, France). All measurements were performed at 25°C after 30 s of equilibration with an
 132 angle detection of 173° backscatter.

133 The size of GSNO-MP was also measured in triplicate in 0.001 M NaCl by a Mastersizer (hydro 2000
 134 SM, Malvern Instruments, France). Span was calculated as follows:

135
$$\text{Span} = (Dv90 - Dv10) / Dv50$$

136 where Dv10, Dv50, Dv90 are values of size below which 10%, 50% or 90% of the particles are
 137 contained.

138 The surface morphology of the particles was investigated by scanning electron microscopy (SEM,
 139 Hitachi S4800, Japan, accelerating voltage 1 kV). Briefly, fresh suspension of GSNO-NP was diluted
 140 10⁶-fold. Then, a drop was deposited and dried overnight at room temperature, and flash carbon
 141 coated (4 s). In the case of GSNO-MP, lyophilizates were observed after carbon coating.

142

143 **2.5. Determination of GSNO encapsulation efficiency (direct method)**

144 The encapsulation efficiency (EE) was determined by quantifying the GSNO contained inside the
 145 particles. After particles centrifugation (42,000 g, 30 min for NP, 10 min for MP), the pellets were
 146 collected and destroyed by methylene chloride. GSNO was then extracted with phosphate buffer
 147 saline (0.148 M PBS, pH=7.4) (ratio methylene chloride/PBS 1:10) using high speed shaking
 148 (2,000 rpm, Heidolph Vibramax 110, Germany). After centrifugation (2,500 g for 10 min), GSNO and
 149 nitrite ions were quantified in the supernatant using Griess-Saville and Griess reactions. GSNO

150 concentration was deduced by subtracting Griess quantification to Griess-Saville quantification.
151 Total recovery of GSNO during the extraction process has been verified and potential matrix effect
152 with polymer residues have been ruled out in preliminary experiments. The encapsulation efficiency
153 was assessed immediately after particles preparation and calculated according to:

$$154 \quad EE = (m_e / m_i) * 100\%$$

155 Where EE is encapsulation efficiency (%), m_e is the mass of drug entrapped in particles, and m_i is the
156 mass of initial drug. The determination of GSNO content inside the particles after lyophilization and
157 during storage was performed using the same protocol (the residual water content of the
158 lyophilizates was considered in the calculations).

159

160 **2.6. Stability of particles before and after lyophilization**

161 After preparation, fresh suspensions of particles were centrifuged (42,000 g, 4°C, NP for 30 min and
162 MP for 10 min). The pellets were re-suspended in 1 mL water and stored at 5±3°C protected from
163 light. After 1, 2, 3, or 4 days, size and GSNO and potential nitrite content of separated aliquots were
164 measured as previously described.

165 After lyophilization, the particle powders were stored at 5±3°C under nitrogen and protected from
166 light. After 1, 2, 3, 4, 5, 8 and 12 weeks, size and GSNO content of separated aliquots were checked
167 as previously described and compared to the values obtained immediately after lyophilization.

168

169 **2.7. Kinetics of GSNO release**

170 Immediately after preparation, 1 mL of fresh particles suspensions were centrifuged (42,000 g, 4°C,
171 30 min for NP and 10 min for MP). The pellets were suspended in 1 mL of 0.148 M PBS (pH 7.4) and
172 transferred into dialysis cellulose membrane (average flat width 10 mm (0.4 in), cut-off 14,000 Da).
173 The membrane was immersed in 200 mL PBS at 37°C protected from light with magnetic agitation at
174 200 rpm. The GSNO and nitrite ions released in the medium were quantified using the DAN and DAN-
175 Hg²⁺ methods at different time intervals (every 30 min during two hours and every hour from two to
176 six hours) [30].

177

178 **2.8. Cytocompatibility of particles**

179 Intestinal Caco-2 cells (ATCC® HTB-37™) were grown in complete medium consisting of Eagle's
180 Minimum Essential Medium supplemented with 10% (v/v) fetal bovine serum (FBS), 4 mM of
181 glutamine, 100 U/mL of penicillin, 100 U/mL of streptomycin, 1% (v/v) of non-essential amino acids.
182 Cells were cultivated at 37°C under 5% CO₂ (v/v) in a humidified incubator. Cells were then seeded in
183 96-well plates at 10⁵ cells/well. After 24 h, cells were exposed to free GSNO (from 25 µM to 2500
184 µM) or to lyophilizate particles (3 batches, in duplicate, at equivalent GSNO concentrations from 25
185 µM to 2500 µM) for 24 h in complete medium. After incubation, cytocompatibility was checked by
186 the 3-(4,5-dimethylthiazol-2-yl)-2,5-diphenyltetrazolium bromide (MTT) method [22]. The
187 absorbance was read at 570 nm with a reference at 630 nm using EL 800-microplate reader (Bio-TEK
188 Instrument, France). Metabolic activity in the presence of treatments was compared to the control
189 condition, i.e. medium alone (as 100%).

190

191 **2.9. Intestinal Permeability**

192 Caco-2 cells were seeded at 2×10^6 cell/cm² on cell culture inserts (Transwell®, Corning, USA) with
193 0.4 μm pore size disposed in a 12-wells plate. Complete medium was replaced every two days during
194 the first week and every day during the second week. The intestinal barrier was validated when the
195 differentiated cell monolayer was obtained after 14-15 days of culture with a transepithelial
196 electrical resistance (TEER) value > 500 Ω.cm². Intestinal permeability of the 3 different lyophilized
197 particles (GSNO concentration 100 μM in all cases, 3 batches, in triplicate) was compared to free
198 GSNO in HBSS containing Ca²⁺ and Mg²⁺ (HBSS+). Two controls of permeability and integrity of the
199 intestinal barrier model using HBSS+ and HBSS without Ca²⁺ and Mg²⁺ (HBSS-) were performed. After
200 1 h of incubation, the amounts of NOx species (i.e. RSNO + nitrite ions + nitrate ions) were quantified
201 using DAN-Hg²⁺, DAN methods with or without nitrate reductase, in the apical compartment both
202 free in the medium and inside the particles, and in the basolateral compartment. A TEER value higher
203 than 300 Ω.cm² and a fluorescein permeability lower than 5% at the end of the test validated the
204 integrity of the intestinal monolayer [22].

205 The apparent permeability coefficients (P_{app}) were calculated as follows:

$$206 P_{app} = (dQ/dt) \times (1/(A \times C_0))$$

207 Where dQ/dt (mol.s⁻¹) refers to the permeability rate (mol) of RSNO or NOx in the basolateral
208 compartment at the time of quantification, A (cm²) to membrane diffusion area, and C₀ (mol.mL⁻¹) to
209 the initial concentration in the apical compartment.

210 The recovery rate of NOx species (mass balance of GSNO) was checked by comparing the amount of
211 NOx species quantified in the different compartments (apical, basolateral, in the particles) with the
212 initial amount of GSNO deposited.

213

214 **2.10. Statistical analysis**

215 All the results are shown as either mean ± standard deviation (sd, for characterization) or mean ±
216 standard error of mean (sem, for cells results). In all cases, three independent batches (preparation
217 and lyophilization) were used.

218 The one-way ANOVA or two-way ANOVA (Dunnett's multiple comparisons test or Tukey's multiple
219 comparisons test) were used for the analysis of particles stability, release and Caco-2 cells
220 experiments. p < 0.05 was considered as significantly different. Statistical analyses were performed
221 using the GraphPad Prism software (GraphPad Software, USA).

222

223 **3. Results and discussion**

224 Currently, pharmacokinetic data of the orally administered GSNO are lacking while its
225 pharmacodynamic effects are well documented and indicate a great therapeutic potential. For
226 example, a recent literature review from Liu et al. [15] highlighted the results obtained with GSNO in
227 clinical trials and preclinical models of stroke: repeated oral administration is used in several of the
228 preclinical studies with promising cerebro-protective or regenerative effects against ischemic lesions,
229 without deciphering the drug transport across the intestinal nor the haemato-encephalic barriers.
230 This absence of information limits the use of GSNO as a therapeutic drug. A pioneer work has been
231 done by Wu et al. [31], whose composite particles promoted GSNO intestinal permeation and led to
232 the formation of releasable NO store in rat aorta 17 h after a single oral administration. However, a

233 lot of work remains to be done to implement data and identify the "best" way to present the drug
234 (*i.e.* drug delivery system) to the intestinal barrier and how it will impact the drug permeability.

235

236 **3.1. Particles size and encapsulation efficiency**

237 The double emulsion/solvent evaporation method is generally suitable for hydrophilic drugs and was
238 previously successfully applied for GSNO encapsulation into Eudragit RLPO [30]. The process applied
239 with two successive ultrasonic emulsifications and methylene chloride evaporation led to a
240 submicronic formulation. However, the encapsulation was still limited and no sustained release was
241 described. The optimization of this formulation process is the challenge of our present study. Starting
242 from the same raw materials (and the same drug/polymer ratio), the initial W/O/W protocol was
243 modified in two ways. On the one hand, the second emulsion step was modified to produce
244 microparticles (GSNO-MPW) instead of nanoparticles (GSNO-NP), as the lower energy emulsification
245 might protect GSNO from degradation. Additionally, the bigger size of the emulsion droplets and
246 resulting particles might both hinder drug leakage during particles preparation and slow down its
247 release from hardened particles [34]. On the second hand, the S/O/W protocol was tested (GSNO-
248 MPS), using GSNO powder instead of GSNO solution in the first emulsion. In comparison to W/O/W
249 processes, S/O/W methods generally improve encapsulation efficiency of hydrophilic or sensitive
250 drugs and can also lead to better release profiles [35-37].

251 In our case, particles size was indeed increased, from $0.225 \pm 0.003 \mu\text{m}$ for GSNO-NP to $69 \pm 7 \mu\text{m}$ for
252 GSNO-MPW and $165 \pm 14 \mu\text{m}$ for GSNO-MPS. However, there was no improvement in the
253 encapsulation efficiency ($28 \pm 2\%$ for GSNO-MPS, $26 \pm 3\%$ for GSNO-MPW, versus $33 \pm 6\%$ for GSNO-
254 NP), corresponding to a drug loading around 0.7% (w drug/w polymer). In all cases, the amount of
255 nitrite ions was negligible ($< \text{limit of quantitation } 0.5 \mu\text{M}$), meaning that the formulation process is
256 suitable for this fragile drug, and that the mild encapsulation efficiency of GSNO is more likely caused
257 by its low entrapment into the polymeric matrices rather than by its degradation.

258

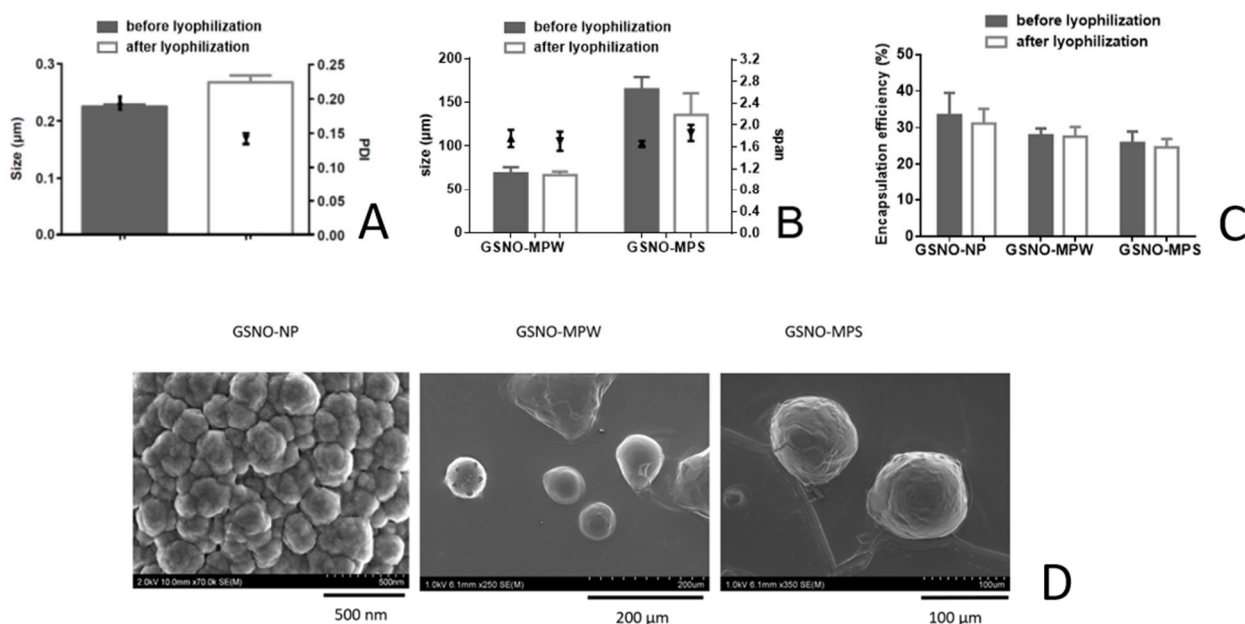
259 In the first step of the S/O/W method, the solid drug is dispersed into an organic solvent. A smaller
260 size of the grain powder facilitates the homogeneous dispersion of the drug, thus improving its final
261 encapsulation [38-39]. Grain size reduction is generally achieved with conventional grinding
262 techniques, but the sensitivity of GSNO to thermal degradation, requires rather innovative
263 supercritical fluid processes [40]. At first, a supercritical antisolvent (SAS 1st trial Table 1) process
264 using DMSO was used. However, it led to a non-acceptable degradation of the drug ($> 70\%$ loss). So,
265 at second, a gaseous anti-solvent (GAS) process was selected, which failed to obtain any solid
266 product, probably because of the too high solubility of GSNO in the CO_2/DMSO mixture, and a too
267 high fraction of DMSO. Finally, the SAS process adapted with milder conditions (2^d trial) led to a pink
268 powder (yield 72%), with more than 80% purity. However, this GSNO powder was too hygroscopic
269 and turned into a sticky product impossible to characterize. This could be due either to a high
270 residual content of DMSO in the powder and/or to the specific features of GSNO, amplified by the
271 higher surface area (reduction of powder particles size with the process). As a result, we used directly
272 the raw GSNO powder in our experiments and dichloromethane as traditional solvent for the 3
273 formulations tested (GSNO-NP, -MPW, -MPS) to compare GSNO intestine absorption in order to
274 conduct a pharmacokinetic approach.

275

276 **3.2. Stability: fresh suspensions versus lyophilized particles**

277 According to the International Conference on Harmonization (ICH) guidelines (Q1A (R2)), a drug
278 product should be evaluated in studies where "the storage conditions and the lengths of studies
279 chosen should be sufficient to cover storage, shipment and subsequent use". For our studies, we
280 choose to store our products at $5 \pm 3^\circ\text{C}$, as a compromise between the thermal fragility of GSNO and

281 an easier storage/shipment. Moreover, due to the very challenging development of GSNO stable
 282 particles, we considered that a 10% (and not 5% as in ICH) change from the initial value will be
 283 considered significant for the critical product attributes, *i.e.* size and GSNO content.
 284 When stored as suspensions, the size of all particles remained stable during three days (not shown).
 285 This can be explained by the electrostatic repulsion between particles allowed by positive charges
 286 (quaternary ammonium groups) brought by Eudragit RLPO polymer (zeta potential of GSNO-NP at
 287 $+38 \pm 1$ mV). However, particles GSNO content dropped to less than 90% of the initial value after one
 288 day, and fell around 60% after two days (not shown) for all suspensions. These results are consistent
 289 with those reported previously for GSNO-NP [30-31].
 290 Lyophilization using 10% w/v sucrose as cryoprotectant was successfully implemented to stabilize the
 291 three particles types (GSNO-NP, -MPW, -MPS) without modifying their critical attributes (Figure 1A,
 292 B, and C). A cryoprotectant was imperative to retain the GSNO content of the particles (no
 293 cryoprotectant = more than 50 % of GSNO lost during freeze-drying), but sucrose was as effective as
 294 trehalose. SEM images show that the particles are roughly spherical, with a more or less smooth
 295 surface and no visible pores at the surface (Figure 1D). It was not possible to observe freeze-dried
 296 powder of GSNO-NP (instead, fresh particles were observed), because the sucrose included in the
 297 lyophilizate generated structures in the same range of size than NP.



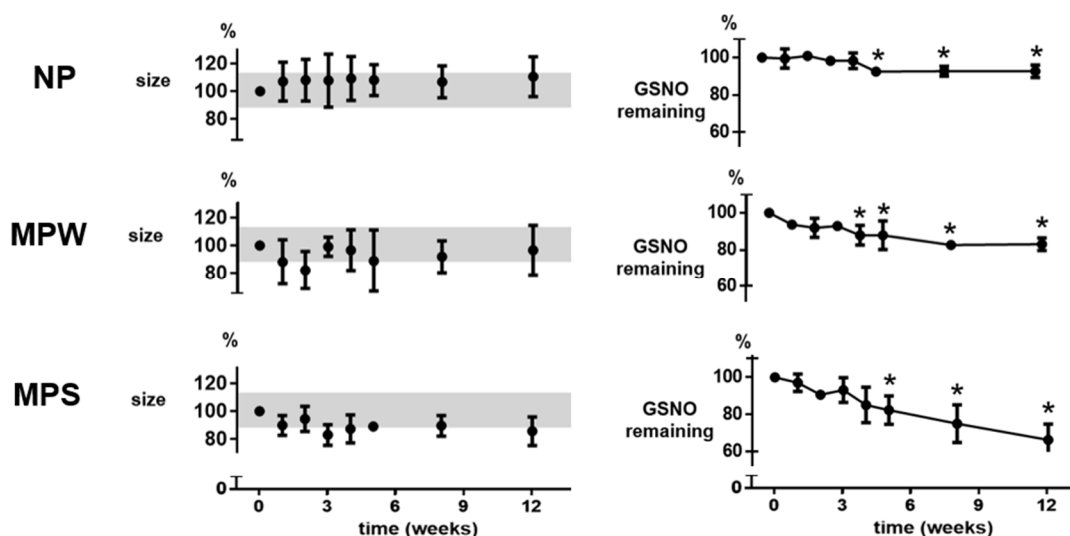
298
 299 **Figure 1: Characterization of GSNO-loaded particles before and after lyophilization.** Size and
 300 polydispersity index (PDI) of the GSNO-NP (A) as well as size and span of the GSNO-MP (B),
 301 encapsulation efficiencies (C) are presented as mean \pm sd (n=3). Representative Scanning Electron
 302 Microscopy images are also presented (D).

303
 304 After lyophilization, size remain stable for the three types of particles during storage for the three
 305 months of study (Figure 2). In contrast, GSNO content decreased significantly after four weeks of
 306 storage for both kinds of microparticles, and more slowly for GSNO-NP (90% of initial content
 307 remaining after three months). These results might be linked to the different residual water content
 308 (w/w) of the lyophilizates, namely $7 \pm 5\%$ for GSNO-NP, $9 \pm 5\%$ for GSNO-MPW and $26 \pm 11\%$ GSNO-
 309 MPS. These values are rather high for freeze-dried formulations (usually $< 2\%$). Either the freeze-

310 drying process was not sufficiently efficient, or the formulations have recaptured water before the
 311 residual water content was measured (this was done as fast as possible, using dessicant to transport
 312 the formulations, but it was not technically feasible to do it in a moisture-controlled environment).
 313 This hygroscopic behavior echoes the one observed previously in the supercritical fluid experiments.
 314 Further investigation of the freeze-drying process might be warranted.

315 However, more than 80% of the initial GSNO amount remained inside GSNO-MPS after one month
 316 and inside GSNO-MPW after two months. This result offers a promising approach for oral delivery
 317 system development.

318



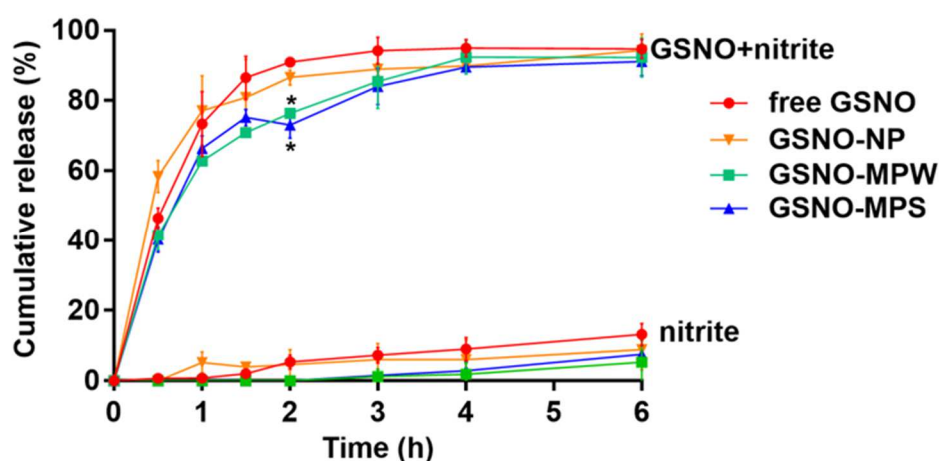
319

320 **Figure 2: Evolution of size and GSNO remaining for the GSNO-NP, GSNO-MPW and GSNO-MPS**
 321 **particles stored at 4 °C under inert atmosphere after lyophilization.** Values measured immediately
 322 after lyophilization are considered as 100%. Results are presented as mean \pm sd (n = 3). The grey
 323 areas delimit the sizes between 90% and 110% of the initial values. For GSNO remaining contents:
 324 one-way ANOVA $p < 0.05$ for the three formulations (Dunnett's multiple comparisons test* $p < 0.05$
 325 versus week 0).

326

327 3.3. In vitro release

328 The kinetic release study was conducted under discriminating conditions (phosphate buffer), with no
 329 ambition of *in vitro/vivo* correlation but to observe the ability of developed drug delivery systems to
 330 protect and release GSNO in a controlled manner. The *in vitro* GSNO release profiles (Figure 3)
 331 showed an initial burst in the first 1.5 h for all types of particles. At 2 h, the cumulative release from
 332 microparticles was lower (around 70-75%) than for free GSNO and GSNO-NP (around 90% released).
 333 Complete release was achieved after 6 h.



334

335 **Figure 3: In vitro drug release.** Results are presented as mean \pm sd (n = 3, free GSNO as control), two-
 336 way ANOVA with $p < 0.05$ for treatments, time and interaction (Tukey's multiple comparisons test: * p
 337 < 0.05 versus free GSNO and GSNO-NP). The cumulative release is presented as total release ("GSNO
 338 + nitrite", i.e. corresponding to the DAN-Hg²⁺ assay, upper curves) or as nitrite ions ("nitrite", lower
 339 curves, DAN assay).

340 In the recent literature, Lautner et al. [41] and Hlaing et al. [25] used S/O/W processes to encapsulate
 341 RSNO into PLGA microparticles. With these polymers, they achieved higher drugs loadings
 342 (respectively 12% for S-nitroso-N-acetylpenicillamine, SNAP, and 5% for GSNO) and sustained release
 343 (several days). With our polymer especially adapted for oral administration, we obtained a 0.7% drug
 344 loading, and a shorter release time, more suited for interaction with the gastrointestinal tract. These
 345 results clearly highlight the challenge to encapsulate GSNO directly into hydrophobic particles
 346 obtained by double emulsion/evaporation. Modifications of the drug (to increase its molecular
 347 weight, for example using phytochelatin, natural polymers of GSNO analogues [42]) or of the
 348 polymer (to graft GSNO directly on the polymer backbone) seem necessary to achieve high drug
 349 loading/sustained release. An attractive alternative strategy mimicking the physiology could be to
 350 encapsulate high molecular weight S-nitrosothiols, which will generate GSNO *in situ* by
 351 transnitrosation of physiological GSH. Previous studies with encapsulation of S-nitroso-N-
 352 acetylcysteine [43] and S-nitroso-captopril [44] proved the effectiveness of this transnitrosation
 353 approach to elicit vasodilation or anti-infectious effects after parenteral or local administration,
 354 respectively.

355 However, despite the lower encapsulation and duration of drug release with our Eudragit particles,
 356 the release rate itself, around 150 pmol. mg⁻¹.min⁻¹ for the first 1.5h, is in the range of previously
 357 described PLGA systems encapsulating NO donors (e.g. from 40 pmol.mg⁻¹.min⁻¹ with SNAP [41] to
 358 400-800 pmol.mg⁻¹.min⁻¹ with DETA NONOate [45]). So, the interaction of particles with a cell model
 359 of intestinal barrier was evaluated.

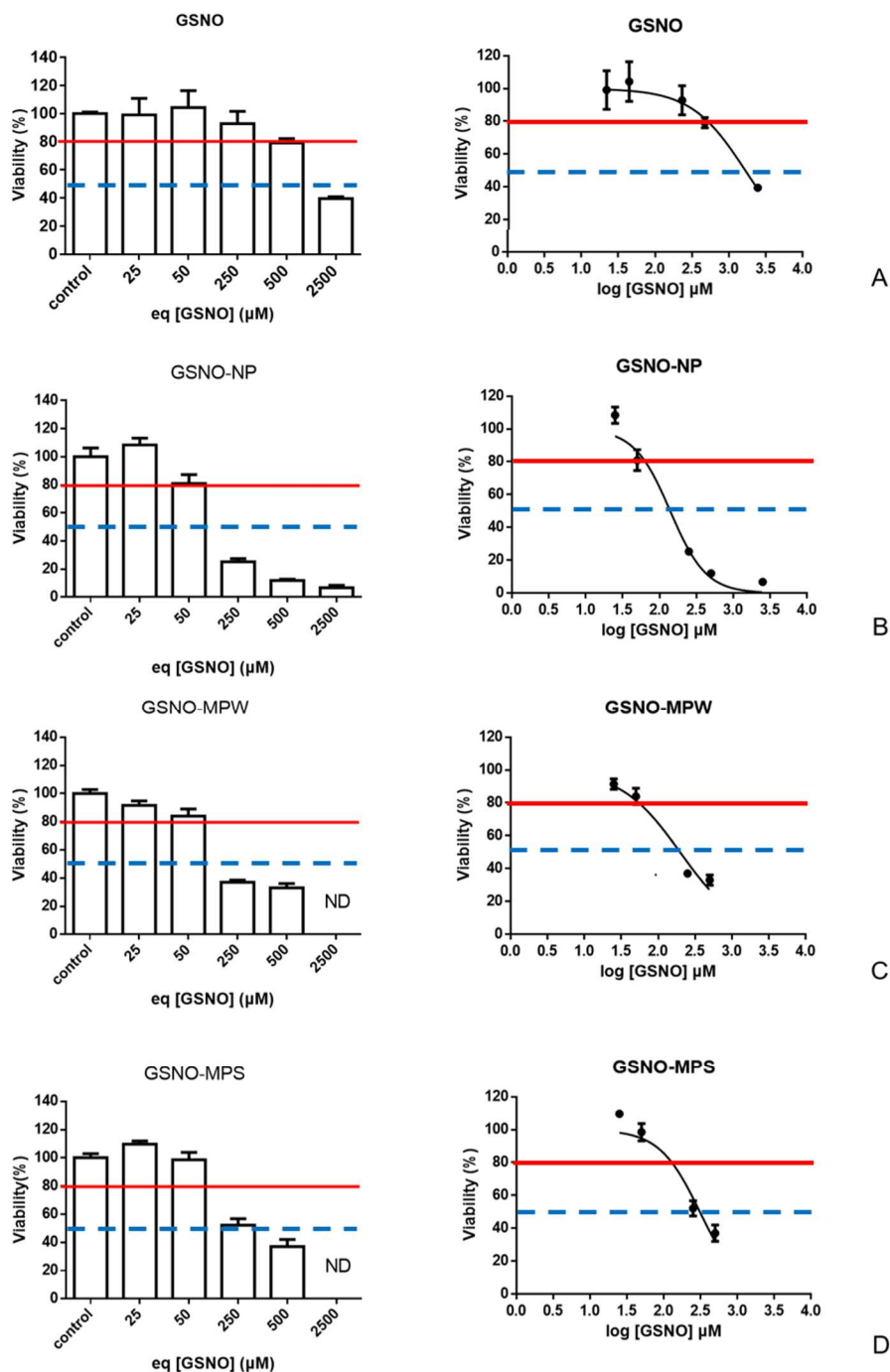
360

361 3.4. Cytocompatibility

362 The 24-h cytocompatibility of the three particle types and free GSNO decreased while increasing the
 363 GSNO concentration (Figure 4). Concentrations tested in this study were deliberately far beyond the
 364 ones needed for physiological effect of GSNO, in order to compare IC₅₀ values of free versus
 365 encapsulated drug. The cell metabolic activity went below 80% for concentrations above 500 μ M for

366 free GSNO, and 50 μM of eq [GSNO] for all particle types. The IC_{50} value of free GSNO ($1718 \pm 1 \mu\text{M}$)
 367 decreased with its encapsulation in GSNO-MPS ($310 \pm 1 \mu\text{M}$), GSNO-MPW ($198 \pm 1 \mu\text{M}$) and GSNO-NP
 368 ($140 \pm 1 \mu\text{M}$).

369



370
 371 **Figure 4: Cytocompatibility of Caco-2 cells after 24 h of incubation with GSNO (A), GSNO-NP (B),**
 372 **GSNO-MPW (C), GSNO-MPS (D). Control condition = culture medium without fetal bovine serum.**
 373 **Results are presented regarding GSNO loading, in equivalence of free GSNO from 25 μM to 2500 μM .**
 374 **Results are shown as means \pm sem, n = 3 in duplicate. ND = not determined**
 375

376 Eudragit RL (R for Retard) are poly(ethylacrylate, methyl methacrylate and methylammonio
 377 ethylmethacrylate copolymers, bearing 8.8–12% quaternary ammonium groups. This material is
 378 commonly employed for pH-independent coating of solid oral drug dosage forms. However, since it is
 379 insoluble in water at physiological pH values and undergoes a certain degree of swelling, it may also
 380 be suitable for the dispersion and controlled oral delivery of actives [46]. The cytocompatibility of
 381 drug delivery based on this polymer is well documented. In this context, the results obtained were
 382 not surprising. However, after oral administration, the concentration of 50 μ M (corresponding
 383 roughly to 2.5 g/L of particles) should not be locally achieved in 24 h but distributed and spread
 384 throughout the length of the intestine. In addition, it is important to note that the study conducted
 385 here was voluntarily conducted on undifferentiated Caco-2 cells, known to be more sensitive than
 386 the cells used for permeability studies (cultured for 15 days prior to the study) [47].

387

388 3.5. Intestinal permeability

389 The intestinal permeability of NO_x species released from particles compared to free GSNO was
 390 evaluated using an *in vitro* intestinal barrier model (Figure 6). Bonetti et al. [22] demonstrated
 391 recently that free RSNO (GSNO, S-nitroso-N-acetylcysteine NACNO and SNAP), without drug delivery
 392 systems, can cross this barrier (Caco-2 model) with a medium apparent permeability rate, using a
 393 passive mode. In the present study, we wanted to explore the ability of Eudragit RL-based-drug
 394 delivery systems to improve GSNO intestine permeability. To follow the future of NO through the
 395 intestinal barrier, it is essential to follow the RSNO but also the degradation products (nitrite ions and
 396 nitrate ions).

397 The mass balance (Table 2) and the values of apparent permeability coefficient (P_{app}) (Table 3) were
 398 then calculated for all NO_x species. The mass balance calculated at the end of the permeability study
 399 showed that most of the GSNO initially encapsulated or added (free) was recovered under RSNO,
 400 nitrite ions and mostly nitrate ions species. Therefore, no NO_x species were produced by cells
 401 attesting for non-stress conditions imposed by the presence of particles.

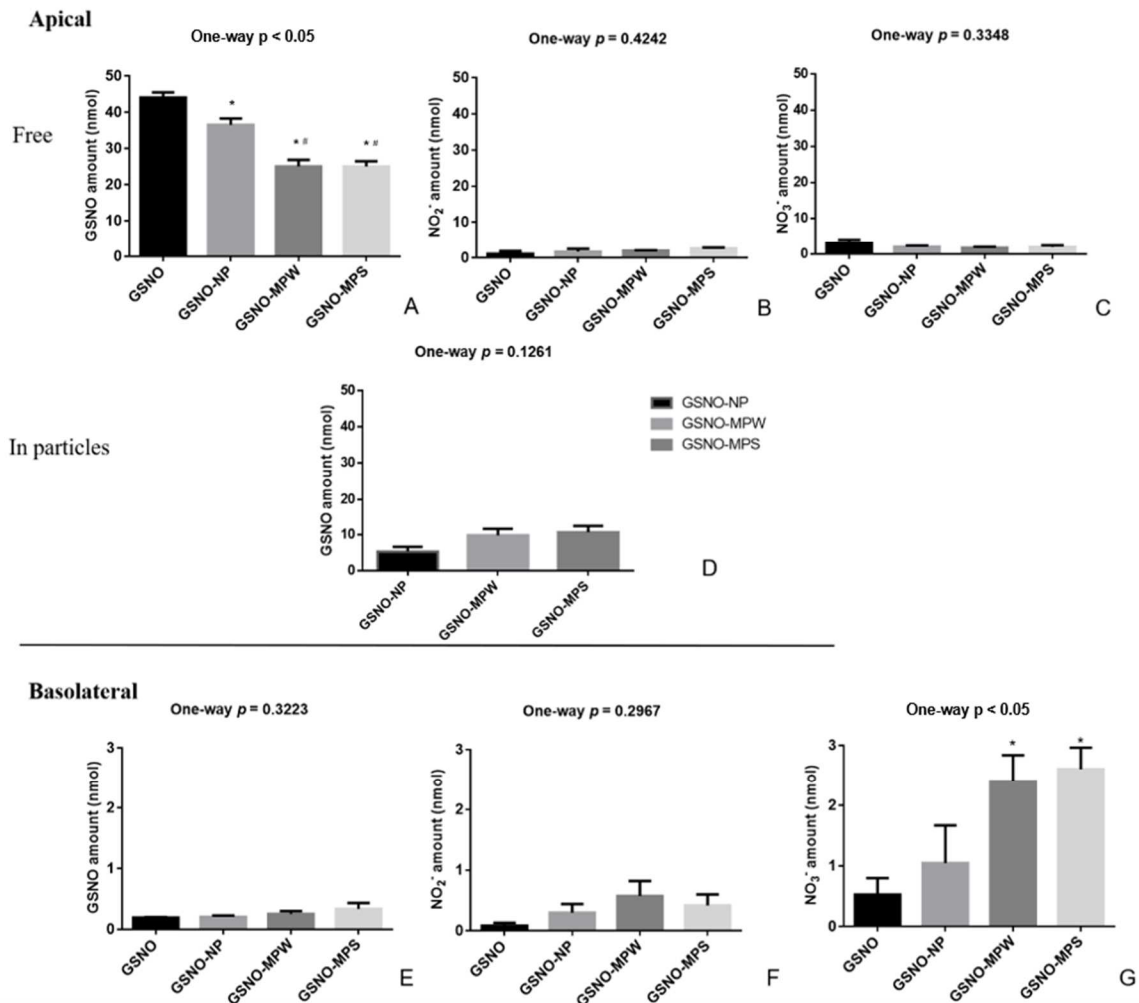
402 **Table 2. Mass balance of NO_x species** for GSNO non-formulated or formulated, after 1 h of
 403 permeability study (GSNO initial amount 50 nmol). Results are presented as mean \pm sem, n=3 in
 404 duplicate, one-way ANOVA on each compartment (Tukey's multiple comparisons test): *p < 0.05
 405 *versus* GSNO.

	Amount in nmol			Total
	Apical		Basolateral	
	Free	In particles		
GSNO	45 \pm 2 (90 \pm 4%)	-	0.8 \pm 0.3 (1.6 \pm 0.6%)	45 \pm 2 (91 \pm 4%)
GSNO-NP	38 \pm 2 (75 \pm 4%)	5 \pm 1 (11 \pm 3%)	1.5 \pm 0.8 (3 \pm 2%)	44 \pm 1 (89 \pm 2%)
GSNO-MPW	32 \pm 3* (62 \pm 6%)	10 \pm 2 (20 \pm 4%)	3 \pm 1 (5 \pm 2%)	43 \pm 1 (85 \pm 2%)

GSNO-MPS	$30 \pm 2^*$ ($60 \pm 5\%$)	11 ± 2 ($21 \pm 4\%$)	2 ± 1 ($5 \pm 2\%$)	43 ± 2 ($86 \pm 4\%$)
-----------------	----------------------------------	--------------------------------	------------------------------	--------------------------------

406

407 At the end of incubation, the amount of GSNO in the apical media was significantly lower for GSNO-
 408 MPW and GSNO-MPS conditions (circa 60% of initial load) than for GSNO-NP (~75%) and free GSNO
 409 (~90%). While around 10% of GSNO remained inside NP, almost 20% were still inside MP. This
 410 confirms the slower release of GSNO for MP than NP, previously observed in the *in vitro* experiment,
 411 which is even slower than in the *in vitro* release study. This can be explained by the bioadhesion
 412 phenomenon, already observed for Eudragit RL, and the establishment of electrostatic interactions
 413 with plasma membranes of Caco-2 cells [46]. In the meantime, both types of MP led to a drastically
 414 higher concentration of nitrate ions (the most permeable NO species) in the basolateral side
 415 compared to free GSNO or NP conditions (Figure 5). Despite the high local concentration of polymer
 416 proposed in this experiment in order to deliver a quantity of RSNO that can be measured, the cells do
 417 not endogenously produce nitrates, as shown by the mass balance (Table 2). As the same amount of
 418 GSNO is contained in the different formulations, this result demonstrates that the same dose of
 419 GSNO delivered by MPs, more localized with a more limited point of contact, results in greater
 420 permeability of the naturally more permeable NO species.
 421



422

423 **Figure 5: Quantity of GSNO, nitrite ions nitrate ions** remaining in the apical medium (A, B and C,
 424 respectively), as well as in the basolateral medium (E, F and G, respectively), and GSNO remaining
 425 inside the particles (D) after 1 h of permeability study (GSNO initial amount = 50 nmol in all cases).
 426 Results are shown as means \pm sem, n=3 in duplicate, one-way ANOVA (Tukey's multiple comparisons
 427 test): *p < 0.05 versus GSNO and # p < 0.05 versus GSNO-NP).

428 The Papp values of each NO species are higher for the two types of GSNO-MP than for GSNO-NP or
 429 free GSNO (Table 3). This led to a global (NOx species) Papp value at least two times higher for GSNO-
 430 MPW and GSNO-MPS than for GSNO-NP and free GSNO. This situation is mainly driven by a higher
 431 permeability of nitrate ions than nitrite ions and RSNO, as previously observed for non-formulated
 432 RSNO [22]. As previously mentioned, this could be simply explained by the different distribution of
 433 particles on the cell surface (between NP or MP). The formation of an embolus, where the dose of
 434 GSNO is focalized on a more limited point of contact with the cell, is favorable to absorption in this *in*
 435 *vitro* model. This phenomenon will probably be different *in vivo* because the intestinal barrier is not
 436 limited to a cell monolayer and mucus also participates in bioadhesion phenomena.

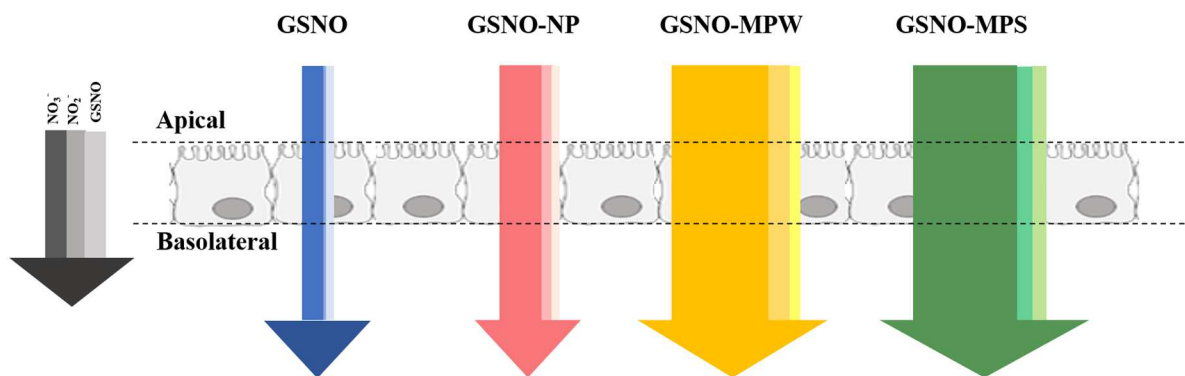
437

438 **Table 3. Values of apparent permeability coefficients (Papp)** for RSNO, nitrite ions, nitrate ions and
 439 NOx (sum of all species) after 1 h of free GSNO, GSNO-NP or GSNO-MPs incubation. Results are
 440 presented as mean \pm sem, n=3 in duplicate.

Treatment	Papp values ($\times 10^{-6}$ cm.s ⁻¹)			
	RSNO	NO ₂ ⁻	NO ₃ ⁻	NOx
GSNO	0.8 \pm 0.4	0.3 \pm 0.2	2.0 \pm 0.2	3.1 \pm 0.6
GSNO-NP	0.6 \pm 0.2	0.9 \pm 0.3	4 \pm 1	6 \pm 2
GSNO-MPW	1.1 \pm 0.7	1.8 \pm 0.3	7 \pm 1	10 \pm 2
GSNO-MPS	1.1 \pm 0.6	1.3 \pm 0.3	8 \pm 2	11 \pm 2

441

442 Indeed, the three types of particles showed an improvement of the intestinal permeability of NOx
 443 species (GSNO-MPS > GSNO-MPW > GSNO-NP) after only 1 h and without damaging the cells
 444 monolayer (Figure 6). The Papp parameter characterizes the intestinal permeability of a drug *in*
 445 *vitro* or *ex vivo* models. Drugs could have low permeability (Papp < 1 $\times 10^{-6}$ cm.s⁻¹) or high
 446 permeability ($\geq 10 \times 10^{-6}$ cm.s⁻¹), or be in a medium permeability class [48]. As a result, considering all
 447 NOx species, GSNO is in the medium permeability class when administered as free GSNO or GSNO-
 448 NP, and reaches the high permeability class using GSNO-MPs ($\geq 10 \times 10^{-6}$ cm.s⁻¹). This data is relevant
 449 and the study shows that, depending on the drug delivery system used, a modulation of GSNO
 450 absorption can be observed.



451
 452 **Figure 6: Graphical summary of NO_x species permeability for each condition** (free GSNO, GSNO-NP,
 453 GSNO-MPW and GSNO-MPS). The width of each section of the arrows is correlated with the amounts
 454 (from left to right) of NO₃⁻, NO₂⁻ and GSNO.
 455

456
 457

4. Conclusion

458 In this study, we overcame the challenge of getting stable and easy-to transport particles for oral
 459 administration of GSNO. Critical parameters of the particles (i.e. size and GSNO content) were
 460 maintained after freeze-drying, and the resulting products were stable at last one month stored at
 461 4°C protected from oxygen. In this way, the lyophilization process has brought a very significant
 462 improvement, since initial suspensions had to be used right after preparation. The discrepancies in
 463 water residual content of the particles after drying indicate that MP (especially the GSNO-MPS ones)
 464 still retain a high amount of water. This might be due to the hygroscopic properties of GSNO powder.
 465 As GSNO is less stable in solution than in dry state, optimization of the lyophilization process could be
 466 conducted in the future in order to reduce residual water content and therefore to improve the
 467 stability of these GSNO-MPS. Microparticles offered a slightly slower *in vitro* release of the drug than
 468 nanoparticles, and led to a better enhancement of NO_x permeability through a model intestinal
 469 barrier. This work confirms the importance of presenting the drug with a suitable delivery system to
 470 the intestine. The NP and MP compared in this study could have different behaviors in *in vivo*
 471 situations and therefore constitute tools for future GSNO oral administration in chronic conditions.

472
 473
 474

References

- [1] Ignarro, L.J., 1999. Nitric oxide as a signaling molecule in the vascular system: an overview. *J. Cardiovasc. Pharmacol.* 34, 879-86. doi:10.1097/00005344-199912000-00016.
- [2] Kuhlencordt P.J., Gyurko R., Han F., Scherrer-Crosbie M., Aretz T.H., Hajjar R., Picard M.H., Huang P.L., 2001. Accelerated atherosclerosis, aortic aneurysm formation, and ischemic heart disease in apolipoprotein E/endothelial nitric oxide synthase double-knockout mice. *Circulation* 104, 448-54. doi:10.1161/hc2901.091399.
- [3] Tonelli A.R., Haserodt S., Aytekin M., Dweik R.A., 2013. Nitric oxide deficiency in pulmonary hypertension: Pathobiology and implications for therapy. *Pulm. Circ.* 3, 20-30. doi:10.4103/2045-8932.109911.
- [4] Momi S., Caracchini R, Falcinelli E, Evangelista S, Gresele P., 2014. Stimulation of platelet nitric oxide production by nebivolol prevents thrombosis. *Arterioscler .Thromb. Vasc. Biol.* 34, 820-9. doi:10.1161/ATVBAHA.114.303290.
- [5] Bienvenu L.A., Morgan J., Reichelt M.E., Delbridge L.M.D., Young M.J., 2017. Chronic in vivo nitric oxide deficiency impairs cardiac functional recovery after ischemia in female (but not male) mice. *J. Mol. Cell. Cardiol.* 112, 8-15. doi:10.1016/j.yjmcc.2017.08.012.
- [6] Hakim T.S., Sugimori K., Camporesi E.M., Anderson G., 1996. Half-life of nitric oxide in aqueous solutions with and without haemoglobin. *Physiol. Meas.* 17, 267-77. doi: 10.1088/0967-3334/17/4/004.
- [7] Zhuge Z., Paulo L.L., Jahandideh A., Brandão M.C.R., Athayde-Filho P.F., Lundberg J.O., Braga V.A., Carlström M.1., Montenegro M.F., 2017. Synthesis and characterization of a novel organic nitrate NDHP: Role of xanthine oxidoreductase-mediated nitric oxide formation. *Redox. Biol.* 13, 163-9. doi: 10.1016/j.redox.2017.05.014.
- [8] Münzel T., Daiber A., 2018. Inorganic nitrite and nitrate in cardiovascular therapy: A better alternative to organic nitrates as nitric oxide donors? *Vascul. Pharmacol.* 102, 1-10. doi: 10.1016/j.vph.2017.11.003.
- [9] Messin R., Boxho G., De Smedt J., Buntinx I.M., 1995. Acute and chronic effect of molsidomine extended release on exercise capacity in patients with stable angina, a double-blind cross-over clinical trial versus placebo. *J. Cardiovasc. Pharmacol.* 25, 558-63. Doi: 10.1097/00005344-199504000-00008.
- [10] Pereira A.C., Araújo A.V., Paulo M., Andrade F.A., Silva B.R., Vercesi J.A., da Silva R.S., Bendhack L.M., 2017. Hypotensive effect and vascular relaxation in different arteries induced by the nitric oxide donor RuBPY. *Nitric Oxide* 62, 11-6. doi: 10.1016/j.niox.2016.11.001.
- [11] Kauser N.I., Weisel M., Zhong Y.L., Lo M.M., Ali A., 2020. Calcium Dialkylamine Diazeniumdiolates: Synthesis, Stability, and Nitric Oxide Generation. *J. Org. Chem.* 85, 4807-12. doi: 10.1021/acs.joc.0c00020.
- [12] Al'Sadoni H., Ferro A., 2000. S-Nitrosothiols: a class of nitric oxide-donor drugs. *Clin. Sci. (Lond).* 98, 507-20. <https://doi.org/10.1042/cs0980507>

- [13] Perrin-Sarrado C., Zhou Y., Salgues V., Parent M., Giummelly P., Lartaud I., Gaucher C., 2020. S-Nitrosothiols as potential therapeutics to induce a mobilizable vascular store of nitric oxide to counteract endothelial dysfunction. *Biochem. Pharmacol.* 173, 113686. doi: 10.1016/j.bcp.2019.113686.
- [14] Gaucher C., Boudier A., Dahboul F., Parent M., Leroy P., 2013. S-nitrosation/denitrosation in cardiovascular pathologies: facts and concepts for the rational design of S-nitrosothiols. *Curr. Pharm. Des.* 19, 458-72. doi: 10.2174/1381612811306030458.
- [15] Liu S., Zheng H., Yu W., Ramakrishnan V., Shah S., Gonzalez L.F., Singh I., Graffagnino C., Feng W., 2020. Investigation of S-Nitrosoglutathione in stroke: A systematic review and meta-analysis of literature in pre-clinical and clinical research. *Exp. Neurol.* 328, 113262. doi: 10.1016/j.expneurol.2020.113262.
- [16] Sliskovic I., Raturi A., Mutus B., 2005. Characterization of the S-denitrosation activity of protein disulfide isomerase. *J. Biol. Chem.* 280, 8733-41. doi:10.1074/jbc.M408080200.
- [17] Stoyanovsky D.A., Tyurina Y.Y., Tyurin V.A., Anand D., Mandavia D.N., Gius D., Ivanova J., Pitt B., Billiar T.R., Kagan V.E., 2005. Thioredoxin and lipoic acid catalyze the denitrosation of low molecular weight and protein S-nitrosothiols. *J. Am. Chem. Soc.* 127, 15815-23. doi: 10.1021/ja0529135.
- [18] Barnett S.D., Buxton I.L.O., 2017. The role of S-nitrosoglutathione reductase (GSNOR) in human disease and therapy. *Crit. Rev. Biochem. Mol. Biol.* 52, 340-54. doi: 10.1080/10409238.2017.1304353.
- [19] Angeli V., Tacito A., Paolicchi A., Barsacchi R., Franzini M., Baldassini R., Vecoli C., Pompella A., Bramanti E., 2009. A kinetic study of gamma-glutamyltransferase (GGT)-mediated S-nitrosoglutathione catabolism. *Arch. Biochem. Biophys.* 481, 191-6. doi: 10.1016/j.abb.2008.10.027.
- [20] Warnecke A., Luessen P., Sandmann J., Ikic M., Rossa S., Gutzki F.M., Stichtenoth D.O., Tsikas D., 2009. Application of a stable-isotope dilution technique to study the pharmacokinetics of human ¹⁵N-labelled S-nitrosoalbumin in the rat: possible mechanistic and biological implications. *J. Chromatogr. B Analyt. Technol. Biomed. Life Sci.* 877, 1375-87. doi: 10.1016/j.jchromb.2008.11.035.
- [21] Yu H., Chaimbault P., Clarot I., Chen Z., Leroy P., 2019. Labeling nitrogen species with the stable isotope ¹⁵N for their measurement by separative methods coupled with mass spectrometry: A review. *Talanta* 191, 491-503. doi: 10.1016/j.talanta.2018.09.011.
- [22] Bonetti J., Zhou Y., Parent M., Clarot I., Yu H., Fries-Raeth I., Leroy P., Lartaud I., Gaucher C., 2018. Intestinal absorption of S-nitrosothiols: Permeability and transport mechanisms. *Biochem. Pharmacol.* 155, 21-31. doi: 10.1016/j.bcp.2018.06.018.
- [23] Duong H.T., Kamarudin Z.M., Erlich R.B., Li Y., Jones M.W., Kavallaris M., Boyer C., Davis T.P., 2013. Intracellular nitric oxide delivery from stable NO-polymeric nanoparticle carriers. *Chem. Commun. (Camb)*. 49, 4190-2. doi : 10.1039/c2cc37181b.
- [24] Parent M., Boudier A., Perrin J., Vigneron C., Maincent P., Violle N., Bisson J.-F., Lartaud I., Dupuis F., 2015. In Situ Microparticles Loaded with S-Nitrosoglutathione Protect from Stroke. *PLoS One* 10, e0144659. doi: 10.1371/journal.pone.0144659.
- [25] Hlaing S.P., Kim J., Lee J., Hasan N., Cao J., Naeem M., Lee E.H., Shin J.H., Jung Y., Lee B.L., Jhun B.H., Yoo J.W., 2018. S-Nitrosoglutathione loaded poly(lactic-co-glycolic acid) microparticles for

prolonged nitric oxide release and enhanced healing of methicillin-resistant *Staphylococcus aureus*-infected wounds. *Eur. J. Pharm. Biopharm.* 132, 94-102. doi: 10.1016/j.ejpb.2018.09.009.

[26] Pelegrino M.T., de Araújo D.R., Seabra A.B., 2018. S-nitrosoglutathione-containing chitosan nanoparticles dispersed in Pluronic F-127 hydrogel: Potential uses in topical applications. *J Drug Deliv Sci Technol* 43, 211-20. <https://doi.org/10.1016/j.jddst.2017.10.016>.

[27] Shah S.U., Martinho N., Socha M., Pinto Reis C., Gibaud S., 2015. Synthesis and characterization of S-nitrosoglutathione-oligosaccharide-chitosan as a nitric oxide donor. *Expert Opin. Drug Deliv.* 12, 1209-23. doi: 10.1517/17425247.2015.1028916.

[28] Shah S.U., Socha M., Fries I., Gibaud S., 2016. Synthesis of S-nitrosoglutathione-alginate for prolonged delivery of nitric oxide in intestines. *Drug Deliv.* 23, 2927-35. doi: 10.3109/10717544.2015.1122676.

[29] Shah S.U., Socha M., Sevil C., Gibaud S., 2017. Spray-dried microparticles of glutathione and S-nitrosoglutathione based on Eudragit® FS 30D polymer. *Ann. Pharm. Fr.* 75, 95-104. doi: 10.1016/j.pharma.2016.09.001

[30] Wu W., Gaucher C., Diab R., Fries I., Xiao Y.L., Hu X.M., Maincent P., Sapin-Minet A., 2015. Time lasting S-nitrosoglutathione polymeric nanoparticles delay cellular protein S-nitrosation. *Eur.J. Pharm. Biopharm.* 89, 1-8. doi: 10.1016/j.ejpb.2014.11.005.

[31] Wu W., Gaucher C., Fries I., Hu X.M., Maincent P., Sapin-Minet A., 2015b. Polymer nanocomposite particles of S-nitrosoglutathione: A suitable formulation for protection and sustained oral delivery. *Int. J. Pharm.* 495, 354-61. doi: 10.1016/j.ijpharm.2015.08.074.

[32] Wu W., Perrin-Sarrado C., Ming H., Lartaud I., Maincent P., Hu X.M., Sapin-Minet A., Gaucher C., 2016. Polymer nanocomposites enhance S-nitrosoglutathione intestinal absorption and promote the formation of releasable nitric oxide stores in rat aorta. *Nanomedicine* 12, 1795-803. doi: 10.1016/j.nano.2016.05.006.

[33] Parent M., Dahboul F., Schneider R., Clarot I., Maincent P., Leroy P., Boudier A., 2013. A complete physicochemical identity card of S-nitrosoglutathione. *Curr. Pharm. Anal.* 9, 31-42. doi: [10.2174/1573412911309010006](https://doi.org/10.2174/1573412911309010006).

[34] Pagels R.F., Prud'homme R.K., 2015. Polymeric nanoparticles and microparticles for the delivery of peptides, biologics, and soluble therapeutics. *J. Control. Release* 219, 519-35. <https://doi.org/10.1016/j.jconrel.2015.09.001>

[35] Chesa-Casalengua P., Jiang C., Bravo-Osuna I., Tucker B.A., Molina-Martinez I.T., Young M.J., Herrero-Vanrell R., 2012. Preservation of biological activity of glial cell line-derived neurotrophic factor (GDNF) after microencapsulation and sterilization by gamma irradiation. *Int. J. Pharm.* 436, 545-54. doi: 10.1016/j.ijpharm.2012.07.019

[36] He J., Li H., Liu C., Wang G., Ge L., Ma S., Huang L., Yan S., Xu X., 2015. Formulation and evaluation of poly(lactic-co-glycolic acid) microspheres loaded with an altered collagen type II peptide for the treatment of rheumatoid arthritis. *J. Microencapsul.* 32, 608-17. doi: 10.3109/02652048.2015.1065924.

[37] Liu J., Xu Y., Liu Z., Ren H., Meng Z., Liu K., Liu Z., Yong J., Wang Y., Li X., 2019. A modified hydrophobic ion-pairing complex strategy for long-term peptide delivery with high drug

- encapsulation and reduced burst release from PLGA microspheres. *Eur. J. Pharm. Biopharm.* 144, 217-29. doi: 10.1016/j.ejpb.2019.09.022
- [38] Zhang Y., Zhang Y., Guo S., Huang W., 2009. Tyrosine kinase inhibitor loaded PCL microspheres prepared by S/O/W technique using ethanol as pretreatment agent. *Int. J. Pharm.* 369, 19-23. doi: 10.1016/j.ijpharm.2008.10.032.
- [39] Han Y., Tian H., He P., Chen X., Jing X., 2009. Insulin nanoparticle preparation and encapsulation into poly(lactic-co-glycolic acid) microspheres by using an anhydrous system. *Int. J. Pharm.* 378, 159-66. doi: 10.1016/j.ijpharm.2009.05.021.
- [40] Jung J., Perrut M., 2001. Particle design using supercritical fluids: Literature and patent survey. *J. Supercrit. Fluids* 20, 179-219. [https://doi.org/10.1016/S0896-8446\(01\)00064-X](https://doi.org/10.1016/S0896-8446(01)00064-X).
- [41] Lautner G., Meyerhoff M.E., Schwendeman S.P., 2016. Biodegradable poly(lactic-co-glycolic acid) microspheres loaded with S-nitroso-N-acetyl-D-penicillamine for controlled nitric oxide delivery. *J. Control. Release* 225, 133-9. doi: 10.1016/j.jconrel.2015.12.056.
- [42] Heikal L., Starr A., Martin G.P., Nandi M., Dailey L.A., 2016. In vivo pharmacological activity and biodistribution of S-nitrosophytochelatin after intravenous and intranasal administration in mice. *Nitric Oxide* 59, 1-9. doi: 10.1016/j.niox.2016.06.006 .
- [43] Nacharaju P., Tuckman-Vernon C., Maier K.E., Chouake J., Friedman A., Cabrales P., Friedman J.M., 2012. *Nitric Oxide* 27, 150-60. doi: 10.1016/j.niox.2012.06.003.
- [44] Mordorski B., Pelgrift R., Adler B., Krausz A., Batista da Costa Neto A., Liang H., Gunther L., Clendaniel A., Harper S., Friedman J.M., Nosanchuk J.D., Nacharaju P., Friedman A.J., 2015. *Nanomedicine* 11, 283-91. doi: 10.1016/j.nano.2014.09.017 .
- [45] Yoo J.W., Lee J.S., Lee C.H., 2010. Characterization of nitric oxide-releasing microparticles for the mucosal delivery. *J. Biomed. Mater. Res. A* 92, 1233-43. doi: 10.1002/jbm.a.32434.
- [46] Paolino D. Vero A., Cosco D., Pecora T.M.G., Ciancolo S., Fresta M., Pignatello R., 2016. Improvement of oral bioavailability of curcumin upon microencapsulation with methacrylic copolymers. *Front. Pharmacol.* 7, 485. doi: 10.3389/fphar.2016.00485.
- [47] Gerloff K., Pereira D.I.A., Faria N., Boots A.W., Kolling J., Förster I., Albrecht C., Powell J.J., Schins R.P.F., 2013. Influence of simulated gastro-intestinal conditions on particle-induced cytotoxicity and interleukin-8 regulation in differentiated and undifferentiated Caco-2 cells. *Nanotoxicology* 7, 353-66. doi: 10.3109/17435390.2012.662249.
- [48] Peng Y., Yadava P., Heikkinen A.T., Parrott N., Railkar A., 2014. Applications of a 7-day Caco-2 cell model in drug discovery and development. *Eur. J. Pharm. Sci.* 56, 120-30. doi: 10.1016/j.ejps.2014.02.008.